UDK: 621.396.96:004.4
COSATI: 17-09

# CATM-CFAR Detector in the Receiver of the Software Defined Radar

Dejan Ivković[1)]
Milenko Andrić[2)]
Bojan Zrnić[3)]
Predrag Okiljević[1)]
Nadica Kozić[1)]

**This paper presents a model of the CATM-CFAR detector in the receiver of the software defined radar. The mentioned detector is named cell-averaging-trimmed-mean CFAR. It is a combination of cell-averaging and trimmed mean CFAR. It is implemented in the receiver of the software defined radar. Some results of a research project related to the design and implementation of the software radar receiver of the conventional radar are presented in this paper. Expressions for the probability of detection, the probability of false alarm and the average decision threshold are derived. The article presents detection of simulated radar targets in Weibull clutter and real radar targets in real clutter and compares the characteristics of the new CATM with some realized well-known CFAR detectors.**

*Key words*: **detector, detection, radar, target acquisition, clutter, receiver, software defined radar.**

## Introduction

RADARS work always in an environment where there are different sources of noise. In addition, there are unwanted signals from other sources of radiation, which can occupy the radar display fully and make targets very hard to see. It must use the adaptive threshold detector, which has a feature that adjusts automatically its sensitivity according to a variety of interference power. Thus it maintains a constant probability of false alarm. A detector with this feature is the constant false alarm rate (CFAR) processor. It is used as a detector in radar receivers to detect targets in the surveillance zone where all of parameters of the statistical distribution of clutter are not known, or where they are non-stationary.

The basic model of the adaptive threshold detector is cell-averaging CFAR (CA-CFAR) [1]. The envelope detector output is the input to the CFAR processor, which is sampled in the range cells. These cells constitute the reference window. The increasing of the number of reference cells induces an increase of the probability of detection ($P_d$). However, there are two basic detection problems associated with the CA-CFAR algorithm. The first problem is the clutter edge and the second problem is the appearance of a multiple target situation. The energy of interference changes rapidly in the case of the clutter edge. For example, this occurs at the border between the land and the sea. A multiple target situation can cause the masking of weaker targets in the neighborhood of stronger targets.

To reduce the negative effects of the two above problems and to preserve the probability of detection at the required level, many modifications of the conventional CA-CFAR have been made. In general, these modifications can be classified into several groups.

The first group consists of CFAR algorithms that use the averaging technique. The smallest-of CFAR (SO-CFAR) [2] is designed to improve target detection in case of multiple target situations. The reference window is divided into a leading part and a lagging part. SO-CFAR selects the part with a smaller sample sum for threshold computation. The greatest-of CFAR (GO-CFAR) [3] is designed to improve target detection in case of the clutter edge. It minimizes the false alarm rate ($P_{fa}$) at a clutter edge by selecting the part with a greater sample sum. The excision CFAR (E-CFAR) [4, 5] provides an excision threshold. The reference cells with amplitudes smaller than an excision threshold are used for detection threshold computation.

The second group consists of algorithms that use the ordering technique, in which, instead of calculating the mean signal in the reference cells, sorting them by the amplitude in the ascending order is carried out. The censored cell-averaging CFAR (CCA-CFAR) [6] is used in the case of a multiple target situation. The reference cells are ordered and only $K$ smallest ranked cells are used for the interference power estimation via the cell-averaging algorithm. Also, the ordered-statistic CFAR (OS-CFAR) [7] is used to resolve problems of multiple target situations. The OS-CFAR forms the detection threshold on the basis of the $k$-th ordered reference cell. The trimmed mean CFAR (TM-CFAR) [8] is a kind of generalization of the original OS-CFAR algorithm where the interference power is estimated as a linear combination of sorted cell content of the observed reference window. TM-CFAR discards $T_1$ smallest ranked cells and $T_2$ greatest ranked cells. After that, the summation of content is done in the remaining reference cells

[1)] Military Technical Institute (VTI), Ratka Resanovića 1, 11132 Belgrade, SERBIA
[2)] University of Defence, Military Academy, Generala Pavla Jurisica Sturma 33, 11000 Belgrade, SERBIA
[3)] Serbian Armed Forces, Defence Technologies Department, Nemanjina 15, 11000 Belgrade, SERBIA

for threshold computation. Also, the generalized ordered statistics CFAR (GOS CFAR) detector [9] represents a modification of the original OS-CFAR. First, the ranked reference cells are weighted with the GOS filter coefficients. The weighted reference cells are used for threshold computation for the design probability of a false alarm rate. The censored mean level CFAR detector (CMLD-CFAR) [10] is used for two correlated targets in the $N$ size reference window. The largest sample is censored. The remaining $N$-1 samples are combined to yield the estimate of the noise level in the cell under test. The automatic censored cell averaging ordered data variability CFAR (ACCA-ODV-CFAR) [11] is used in a situation when the number of interferences and clutter cells is unknown. The algorithm determines the number of $P$ smallest cells which can be considered as homogenous environment. The detection threshold is calculated on the basis of $P$ selected cells. The optimal censored mean level CFAR detector (Opt-CMLD-CFAR) [12] is proposed for multiple target situations. It is based on an optimal selection of the appropriate censored mean level according to the actual background environment. The Opt-CMLD-CFAR has $M$ channels per azimuth for non-coherent integration. The ordered data variability (ODV) algorithm is used to obtain the level of interference power in the test cell and to select the scaling factor of the detection threshold for the design probability of false censoring (PFC).

The third group consists of some algorithms which are a combination of the above mentioned techniques, also in order to reduce problems of the clutter edge and interfering targets. In [13, 14], a combination of the smallest-of and greatest-of concepts with OS-CFAR is proposed. The ordered-statistics smallest-of CFAR (OSSO-CFAR) is considered as a solution to the problem of multiple target situations. The ordered-statistics greatest-of CFAR (OSGO-CFAR) is used to solve the problem of the clutter edge. The cost, paid by the introduction of OSGO and OSSO detectors, is a decrease of the probability of detection in homogenous clutter. The weighted order statistic and fuzzy rules CFAR (WOSF-CFAR) [15] detector uses some soft rules based on fuzzy logic to cure the mentioned problems by OSSO and OSGO-CFAR detectors. The WOSF-CFAR has various combining functions such as algebraic product (AP), algebraic sum (AS), Einstein product (EI), maximum (MAX) and minimum (MIN) to produce some soft weighting function for the decision on the target presence.

The fourth group consists of algorithms that in their procedures have some kind of a fusion center. This group can be divided into two subgroups on the basis of the implementation method of data fusion. The first subgroup consists of models which practice data fusion from several distributed CFAR detectors in space. In [16], a review of different distributed CFAR detection techniques is presented. Distributed fuzzy CA-CFAR and OS-CFAR detectors [17] which use the AP operator give better results than the binary AND and binary OR for homogenous environment as well as in multiple target or clutter edge situations. The evolutionary algorithms (EAs) are applied for threshold optimization in distributed OS-CFAR detectors [18] by using AND and OR fusion rules. The results show that EAs-OS-CFAR detectors are very flexible for solving of optimization problems in CFAR systems. The fuzzy cell-averaging CFAR (FCA-CFAR) and the fuzzy greatest-of CFAR (FGO-CFAR) [19] detectors are applied in a decentralized fuzzy fusion data center to improve a probability of targets detection in the presence of the homogenous Pearson distributed clutter. The fusion data center has $L$ distributed fuzzy CFAR detectors and it uses MAX, MIN, AS and AP fuzzy rules for threshold optimization. The second subgroup consists of models which practice data fusion by using a parallel operation of several CFAR detectors centralized in one sensor. The linear combination of order statistics CFAR (LCOS-CFAR) [20] detector has the $M$ channeled reference window, which can become CA, CCA, OS or TM-CFAR detector for some specific parameter values. The algorithm implies a noncoherent integration of M pulses. The LCOS-CFAR detector orders cells in each channel of the reference window and then trims $T_1$ samples from the lower and $T_2$ samples from the upper end, and then sums the remaining samples to estimate the interference power in the cell under test. The And-CFAR and Or-CFAR [21] use binary AND and binary OR to make data fusion from CA-CFAR and OS-CFAR detectors which work in parallel. An algorithm of parallel operation of CA, GO and SO-CFAR detectors with one fusion center based on neural network [22] provides a better probability of detection than single conventional CA, GO or SO-CFAR algorithms. Also, an algorithm of parallel operation of CA, TM and OS-CFAR detectors [23] with some data fusion rules provides a better final decision than single conventional CA, TM or OS-CFAR algorithms in multiple target situations.

In this paper, we describe a CFAR detector named cell-averaging-trimmed-mean CFAR (CATM-CFAR), which is a combination of CA-CFAR and TM-CFAR. This CFAR has some advantages over other types of CFAR detectors. The paper is organized as follows. The model description that has been used to analyze the performance of the CATM-CFAR detector is discussed in the second part. In the third part, a description of CATM-CFAR is given, and exact expressions for the parameters of a new CFAR detector are derived. Also, a comparison of the CATM-CFAR with several other models of CFAR detector is done. The simulation results of multiple target detection in Weibull and real clutter are showed in the fourth part. Finally, in the fifth part, we gave some conclusions.

## Model description

The block diagram of a typical CFAR detector is shown in Fig.1. The reference window consists of $N$+1=2$n$+1 reference cells. The cell $Y$ in the middle of the reference window is a cell under test. Envelope detector output samples are sent serially into the reference window. The first step is to calculate the mean clutter power level $Z$ using the appropriate CFAR algorithm.

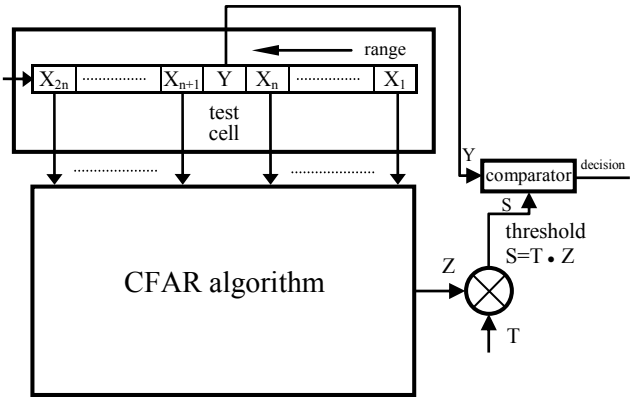


**Figure 1.** Typical CFAR detector

The second step is to multiply $Z$ by a scaling factor $T$ which depends on the CFAR algorithm and the designed probability of the false alarm rate $P_{fa}$. The product $TZ$ is the

detection threshold $S$. The CA-CFAR and TM-CFAR algorithms are interesting for this paper. Fig. 2 shows the CA-CFAR detector scheme which consists of two summers for the leading and lagging windows. Here, $Z$ is simply the sum of $Y_1$ and $Y_2$. Fig. 3 shows the TM-CFAR detector scheme. The first cells in the reference window are sorted per amplitude. Then it trims $T_1$ smallest cells and $T_2$ cells with the highest amplitudes. After that, the summation of the content in the remaining cells is done to obtain $Z$.

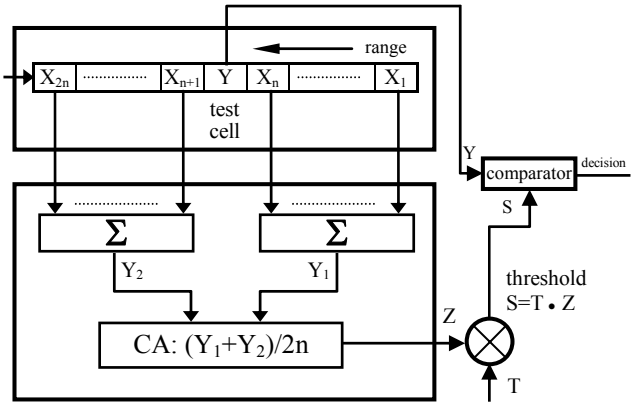


**Figure 2.** CA-CFAR detector

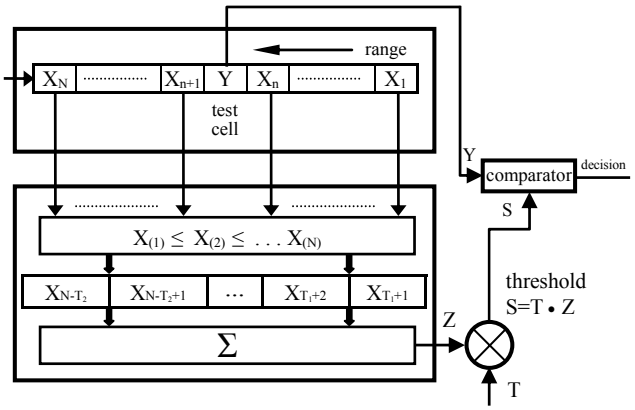


**Figure 3.** TM-CFAR detector

In this paper, we assume that in homogenous clutter envelope detector output samples are all exponentially distributed with the probability density function (pdf):

$$f(x) = \frac{1}{2\lambda} e^{-\frac{x}{2\lambda}} \tag{1}$$

where $\lambda$ is the reflected radar signal power. Therefore, we assumed Swerling I model for reflected radar signals from a target. Also, it is assumed that the values in all reference cells and the cell under test are statistically independent. Under the hypothesis $H_0$ when the target is not present in the cell under test, $\lambda$ is the background clutter power $\mu$. Under the hypothesis $H_1$ when the target is present in the cell under test, $\lambda$ is $\mu(1+SNR)$, where $SNR$ is the signal-to-noise ratio of a target. The value $\lambda$ for the cell under test can be expressed:

$$\lambda = \begin{cases} \mu & , \text{ under } H_0 \\ \mu(1+SNR) & , \text{ under } H_1 \end{cases} \tag{2}$$

In digital processing of radar signals, it is not possible to use an optimal detector with the fixed optimal threshold $S_O$ to decide about target presence. One reason for that is a priori unknown background clutter power. Therefore, a solution for this real problem is to use the CFAR detector which has a constant probability of false alarm. For the optimal detector with the fixed optimal threshold $S_O$, $P_{fa}$ is given by:

$$P_{fa} = P\left[Y > S_O \mid H_0\right] = e^{-\frac{S_O}{2\mu}} \tag{3}$$

Similarly, the probability of detection for the optimal detector $P_{dO}$ is:

$$P_{dO} = P\left[Y > S_O \mid H_1\right] = e^{-\frac{S_O}{2\mu(1+SNR)}} \tag{4}$$

Combining (3) and (4) we can get another form for $P_{dO}$:

$$P_{dO} = e^{-\frac{S_O}{2\mu}\frac{1}{1+SNR}} = \left(e^{-\frac{S_O}{2\mu}}\right)^{\frac{1}{1+SNR}} \tag{5}$$

$$P_{dO} = P_{fa}^{(1+SNR)^{-1}} \tag{6}$$

In the CFAR detector, the threshold $S$ changes its amount according to the random variable $Z$. The distribution of the $Z$ depends on the chosen CFAR algorithm and the instantaneous content of all cells in the reference window. Generally, by CFAR detectors $P_{fa}$ is:

$$P_{fa} = E_Z\left(P\left[Y > S \mid H_0\right]\right) \tag{7}$$

where $E_Z$ is the operator for expectation of the random variable $Z$. It can be written that $P_{fa}$ is also:

$$P_{fa} = E_Z\left(\int_{TZ}^{\infty} \frac{1}{2\mu} e^{-\frac{y}{2\mu}} dy\right) \quad , \quad S = TZ \tag{8}$$

$$P_{fa} = E_Z\left(e^{-\frac{TZ}{2\mu}}\right) \tag{9}$$

According to [8], it follows that for CFAR detectors $P_{fa}$ is:

$$P_{fa} = M_Z\left(\frac{T}{2\mu}\right) \tag{10}$$

where $M_Z$ is the operator for the moment generating function (mgf) of the random variable $Z$. Similarly, the probability of detection for CFAR detectors can be expressed as:

$$P_d = E_Z\left(P\left[Y > S \mid H_1\right]\right) \tag{11}$$

$$P_d = E_Z\left(P\left[Y > TZ \mid H_1\right]\right) \quad , \quad S = TZ \tag{12}$$

We can determine the finite form for $P_d$ by replacing $\mu$ with $\mu(1+SNR)$ in (10):

$$P_d = M_Z\left(\frac{T}{2\mu(1+SNR)}\right) \tag{13}$$

For comparing different CFAR algorithms, we can use the average decision threshold ($ADT$). According to [7, 8] $ADT$ can be calculated as:

$$ADT = \frac{E(TZ)}{2\mu} = T \cdot \frac{E(Z)}{2\mu} \tag{14}$$

By CFAR, it can be written that [8]:

$$\frac{E(Z)}{2\mu} = -\frac{dM_Z\left(\frac{T}{2\mu}\right)}{dT}\bigg|_{T=0} \tag{15}$$

By replacing (10) in (15) we get:

$$\frac{E(Z)}{2\mu} = -\frac{dP_{fa}}{dT}\bigg|_{T=0} \tag{16}$$

The finite form of the average decision threshold for some CFAR algorithm can be written as:

$$ADT = -T \cdot \frac{dP_{fa}}{dT}\bigg|_{T=0} \tag{17}$$

For the required $P_{fa}$ value, we can compare two different CFAR detectors by the ratio of their average decision thresholds measured in dB as [7]:

$$\Delta = 10\log\frac{ADT_1}{ADT_2} \tag{18}$$

If $\Delta$ is negative, that means that the first CFAR detector has smaller loss in the homogenous clutter background than the second CFAR. Also, we may calculate an approximate signal-to-noise ratio loss $\Delta_O$ for some CFAR detector for a required probability of detection $P_d$. By replacing $S_O/2\mu$ in (4) with *ADT* of a CFAR detector, we get a needed value of the *SNR* of the used CFAR detector ($SNR_n$) for the required probability of false alarm and the probability of detection as:

$$SNR_n = -\left(1+\frac{ADT}{\ln P_d}\right) \tag{19}$$

The needed value of the *SNR* of the optimal detector ($SNR_O$) for the required probability of false alarm and the probability of detection is calculated from (6) as:

$$SNR_O = \frac{\ln P_{fa}}{\ln P_d} - 1 \tag{20}$$

According to [8], and expressions (19) and (20), we can write that the approximate signal-to-noise ratio loss measured in dB is:

$$\Delta_O = 10\log\left(\frac{SNR_n}{SNR_O}\right) = 10\log\left(\frac{1+\frac{ADT}{\ln P_d}}{1-\frac{\ln P_{fa}}{\ln P_d}}\right) \tag{21}$$

$$\Delta_O = 10\log\left(\frac{\ln P_d + ADT}{\ln P_d - \ln P_{fa}}\right) \tag{22}$$

Expression (22) is universal and it can be used for all available CFAR models. The smallest signal-to-noise ratio loss has the CFAR detector with the smallest average decision threshold.

## The CATM-CFAR detector

The novel cell-averaging-trimmed-mean CFAR (CATM-CFAR) optimizes good features of some mentioned CFAR detectors from different groups depending on the characteristics of clutter and present targets with the goal of increasing the probability of detection at a constant probability of false alarm rate. It is realized by the parallel operation of two types of CFAR detectors: CA-CFAR and TM-CFAR. Its structure is showed in Fig.4.

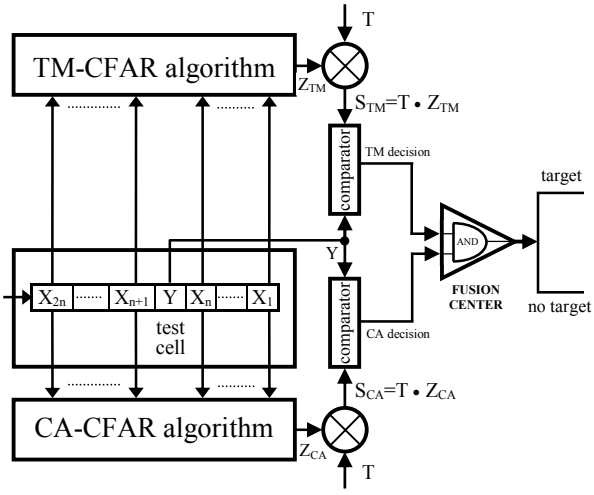


**Figure 4.** Block diagram of the CATM-CFAR detector

The CA-CFAR detector and the TM-CFAR detector work simultaneously and independently but with the same scaling factor of the detection threshold *T*. They produce their own mean clutter power level *Z* using the appropriate CFAR algorithm. Next, they calculate their own detection thresholds $S_{CA}$ and $S_{TM}$. After the comparison with the content in the cell under test *Y*, they decide about target presence independently. The finite decision about target presence is made in the fusion center composed of one "and" logic circuit. If both input single decisions in the fusion center are positive, the finite decision of the fusion center is the presence of the target in the cell under test. In other cases, the finite decision is negative and the target is not at the location which corresponds with the cell under test.

*A) Probability of false alarm and probability of detection*

In each CFAR algorithm, the probability of false alarm should be a constant value. This fact is considered by CATM-CFAR as well. Since single decisions about the target presence of CA and TM parts of the CATM-detector are independent events, according to [24], both the probability of false alarm $P_{faCATM}$ and the probability of detection $P_{dCATM}$ for CATM-CFAR can be written as:

$$P_{faCATM} = P_{faCA} \cdot P_{faTM} \tag{23}$$

$$P_{dCATM} = P_{dCA} \cdot P_{dTM} \tag{24}$$

where $P_{faCA}$ and $P_{faTM}$ are the probability of false alarm of CA and TM parts respectively, $P_{dCA}$ and $P_{dTM}$ are the probability of detection of CA and TM parts respectively.

The random variable which represents the mean clutter power level $Z_{CA}$ is:

$$Z_{CA} = \frac{\sum_{i=1}^{N} X_i}{N} \tag{25}$$

where $X_i$ is the signal amplitude in the i-th cell of the reference window. The probability of false alarm $P_{faCA}$ can be expressed [1]:

$$P_{faCA} = (1+T)^{-N} \tag{26}$$

By replacing *T* in (26) with *T*/(*1*+*SNR*) we get the probability of detection $P_{dCA}$ as:

$$P_{dCA} = \left(1+\frac{T}{1+SNR}\right)^{-N} \tag{27}$$

According to (17), we get the average decision threshold for the CA-CFAR algorithm $ADT_{CA}$. We have that:

$$\frac{dP_{faCA}}{dT} = -\frac{N}{(1+T)^{N+1}} \tag{28}$$

Assuming that $T$=0, we get:

$$\left.\frac{dP_{faCA}}{dT}\right|_{T=0} = -N \tag{29}$$

By replacing (29) into (17), $ADT_{CA}$ is:

$$ADT_{CA} = TN \tag{30}$$

The random variable which represents the mean power level $Z_{TM}$ is [8]:

$$Z_{TM} = \sum_{j=T_1+1}^{N-T_2} X_j \tag{31}$$

To obtain the finite value for $Z_{TM}$, we introduced a new random variable $W$ which is defined as the following column vector:

$$W = \begin{bmatrix} W_1 = X_{T_1+1} \\ W_2 = X_{T_1+2} - X_{T_1+1} \\ \cdot \\ \cdot \\ \cdot \\ W_{N-T_1-T_2} = X_{N-T_2} - X_{N-T_2-1} \end{bmatrix} \tag{32}$$

The random variable $W$ is multiplied with a determined coefficient and the result is a new random variable $V$ defined as:

$$V_i = (N-T_1-T_2-i+1)W_i, \quad i = 1,2,...,N-T_1-T_2 \tag{33}$$

The random variable $V$ is used directly to estimate the random variable $Z$ as:

$$Z = \sum_{i=1}^{N-T_1-T_2} V_i \tag{34}$$

The probability of false alarm $P_{faTM}$ can be calculated as [8]:

$$P_{faTM} = \prod_{i=1}^{N-T_1-T_2} M_{V_i}(T) \tag{35}$$

$$M_{V_1}(T) = \frac{N!}{T_1!(N-T_1-1)!(N-T_1-T_2)} \cdot \sum_{j=0}^{T_1} \frac{\binom{T_1}{j}(-1)^{T_1-j}}{\frac{N-j}{N-T_1-T_2}+T} \tag{36}$$

$$M_{V_i}(T) = \frac{a_i}{a_i+T}, \quad i = 2,3,...,N-T_1-T_2 \tag{37}$$

where $a_i$ is defined as:

$$a_i = \frac{N-T_1-i+1}{N-T_1-T_2-i+1} \tag{38}$$

By replacing $T$ in (35), (36) and (37) with $T/(1+SNR)$ we get the probability of detection $P_{dTM}$ as:

$$P_{dTM} = \prod_{i=1}^{N-T_1-T_2} M_{V_i}\left(\frac{T}{1+SNR}\right) \tag{39}$$

According to (17), we get the average decision threshold for the TM-CFAR algorithm $ADT_{TM}$. Assuming that $T$=0, according to [8], it follows that:

$$\left.\frac{dP_{faTM}}{dT}\right|_{T=0} = -\frac{N!}{(N-T_1-1)!}\sum_{j=0}^{T_1}\frac{(-1)^{T_1-j}}{(N-j)\,j!(T_1-j)!}\cdot \left[\frac{N-T_1-T_2}{N-j}+\sum_{i=2}^{N-T_1-T_2}\frac{1}{a_i}\right] \tag{40}$$

By replacing (40) into (17) $ADT_{TM}$ is:

$$ADT_{TM} = \frac{TN!}{(N-T_1-1)!}\sum_{j=0}^{T_1}\frac{(-1)^{T_1-j}}{(N-j)\,j!(T_1-j)!}\cdot \left[\frac{N-T_1-T_2}{N-j}+\sum_{i=2}^{N-T_1-T_2}\frac{1}{a_i}\right] \tag{41}$$

Now we can write a formula for the probability of false alarm of a CATM-CFAR by replacing (26) and (35) into (23) as:

$$P_{faCATM} = (1+T)^{-N}\prod_{i=1}^{N-T_1-T_2} M_{V_i}(T) \tag{42}$$

Similarly, by replacing (27) and (39) into (24) we get the expression for the probability of detection of a CATM-CFAR detector as:

$$P_{dCATM} = \left(1+\frac{T}{1+SNR}\right)^{-N}\prod_{i=1}^{N-T_1-T_2} M_{V_i}\left(\frac{T}{1+SNR}\right) \tag{43}$$

To get a formula for the average decision threshold of the CATM-CFAR detector $ADT_{CATM}$ , we differentiate (42) and get the following expression:

$$\frac{dP_{faCATM}}{dT} = \frac{d\left((1+T)^{-N}\right)}{dT}\cdot\prod_{i=1}^{N-T_1-T_2} M_{V_i}(T) + \frac{d\left(\prod_{i=1}^{N-T_1-T_2} M_{V_i}(T)\right)}{dT}\cdot(1+T)^{-N} \tag{44}$$

Assuming that $T$=0, we have that:

$$\left.\frac{dP_{faCATM}}{dT}\right|_{T=0} = -N-\frac{N!}{(N-T_1-1)!}\sum_{j=0}^{T_1}\frac{(-1)^{T_1-j}}{(N-j)\,j!(T_1-j)!}\cdot \left[\frac{N-T_1-T_2}{N-j}+\sum_{i=2}^{N-T_1-T_2}\frac{1}{a_i}\right] \tag{45}$$

By replacing (45) into (17) $ADT_{CATM}$ is:

$$ADT_{CATM} = TN+\frac{TN!}{(N-T_1-1)!}\sum_{j=0}^{T_1}\frac{(-1)^{T_1-j}}{(N-j)\,j!(T_1-j)!}\cdot \left[\frac{N-T_1-T_2}{N-j}+\sum_{i=2}^{N-T_1-T_2}\frac{1}{a_i}\right] \tag{46}$$

Following expressions (30), (41) and (46), we can derive that $ADT_{CATM}$ is:

$$ADT_{CATM} = ADT_{CA} + ADT_{TM} \tag{47}$$

*B) Analysis of the CATM-CFAR detector*

In this section, we analysed the performances of the CATM-CFAR detector. We also compared its features with the features of some other CFAR detectors. For the reason of comparison with the results showed in [8], $P_{fa}$ has a value of $10^{-6}$ and the size of the reference window $N$ has a value of 24. The parameter $k$ of OS-CFAR has a value of 18. Both parameters for trimming, $T_1$ and $T_2$, have a value of 3. For this case, the calculated values of the scaling factor of the detection threshold $T$, the average decision threshold $ADT$ and the approximate signal-to-noise ratio loss $\Delta_O$ (according to (22)) for the mentioned CFAR detectors are listed in Table 1. The signal-to-noise ratio loss of the CATM-CFAR has the smallest value of 0.745 dB.

**Table 1.** Approximate signal-to-noise ratio loss $\Delta_0$

| CFAR | $T$ | $ADT$ | $\Delta_O$ [dB] |
|---|---|---|---|
| CATM | 0.418 | 16.2702 | 0.745 |
| CAOS | 0.712 | 18.0235 | 1.208 |
| CA | 0.779 | 18.6960 | 1.373 |
| TM | 1.327 | 19.7933 | 1.630 |
| OS | 16.293 | 21.6041 | 2.024 |

Note: $P_d$=0.5, $P_{fa}$=$10^{-6}$, $N$=24, $k$=18, $T_1$=3, $T_2$=3, $SNR_O$=12.772 dB.

The probabilities of detection of the optimal detector and CATM, CAOS (And-CFAR from [21]), CA, TM and OS CFAR detectors as a function of the signal-to-noise ratio for the parameter values from Table 1 are shown in Fig.5. It can be seen that the detection curve of the CATM-CFAR is the nearest to the detection curve of the theoretically optimal detector.

If you select a field of about $P_d$=0.5, an experimental confirmation of the data from Table 1 is obtained. This is shown in Fig.6 for optimal, CATM, CA, TM and OS-CFAR detectors.

Table 2 lists the scaling factor of the detection threshold $T$ and the average decision threshold $ADT_{CATM}$ of the CATM-CFAR detector for symmetric and asymmetric trimming for $P_{faCATM}$=$10^{-6}$ and $N$=24. The values of $T$ are calculated iteratively from (42) for the given values of $T_1$ and $T_2$. The values of $ADT_{CATM}$ are computed from (47).

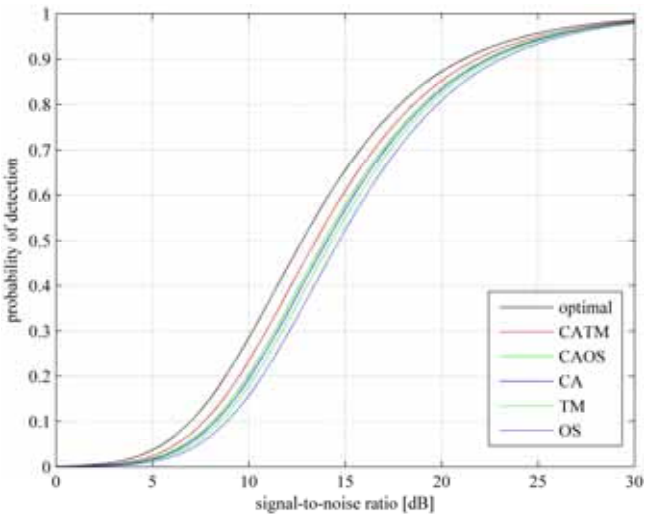


**Figure 5.** Detection curves for the proposed CFAR detectors ($P_{fa}$=$10^{-6}$, $N$=24)

As the trimming increases, both $T$ and $ADT_{CATM}$ increase. But this increase is smaller than the appropriate $T$ and $ADT$ increases of TM-CFAR from Table 4 in [8]. This is shown in Fig.7 for symmetric trimming ($T_1$=$T_2$). For each value of symmetric trimming points, $T$ and $ADT$ of CATM-CFAR are smaller than the appropriate $T$ and $ADT$ of TM-CFAR. Also, the changes of $T$ and $ADT$ for asymmetric trimming by CATM-CFAR are minor in comparison to similar changes by TM-CFAR. This is demonstrated in Fig.8 and Fig.9 as well.

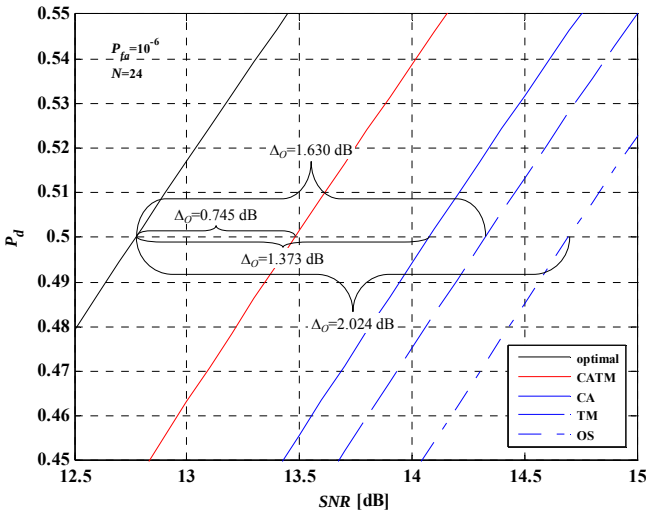


**Figure 6.** Selected detection curves for the proposed CFAR detectors

**Table 2.** Scaling factor T and the average decision threshold ADT of the CATM-CFAR detector

| Symmetric trimming | | | | Asymmetric trimming | | | |
|---|---|---|---|---|---|---|---|
| $T_1$ | $T_2$ | $T$ | $ADT_{CATM}$ | $T_1$ | $T_2$ | $T$ | $ADT_{CATM}$ |
| 0 | 0 | 0.333 | 16.0090 | 2 | 4 | 0.441 | 16.3708 |
| 1 | 1 | 0.364 | 16.0833 | 2 | 7 | 0.513 | 16.7155 |
| 2 | 2 | 0.391 | 16.1727 | 2 | 10 | 0.582 | 17.1159 |
| 3 | 3 | 0.418 | 16.2702 | 2 | 15 | 0.687 | 17.8563 |
| 4 | 4 | 0.445 | 16.3770 | 2 | 17 | 0.721 | 18.1440 |
| 5 | 5 | 0.473 | 16.4956 | 2 | 20 | 0.761 | 18.5099 |
| 6 | 6 | 0.502 | 16.6312 | 4 | 2 | 0.394 | 16.1757 |
| 7 | 7 | 0.534 | 16.7900 | 7 | 2 | 0.403 | 16.1890 |
| 8 | 8 | 0.569 | 16.9822 | 10 | 2 | 0.418 | 16.2241 |
| 9 | 9 | 0.608 | 17.2246 | 14 | 2 | 0.455 | 16.3449 |
| 10 | 10 | 0.653 | 17.5453 | 17 | 2 | 0.506 | 16.5728 |
| 11 | 11 | 0.708 | 17.9952 | 20 | 2 | 0.609 | 17.2001 |

Note: $P_{faCATM}$=$10^{-6}$ and $N$=24.

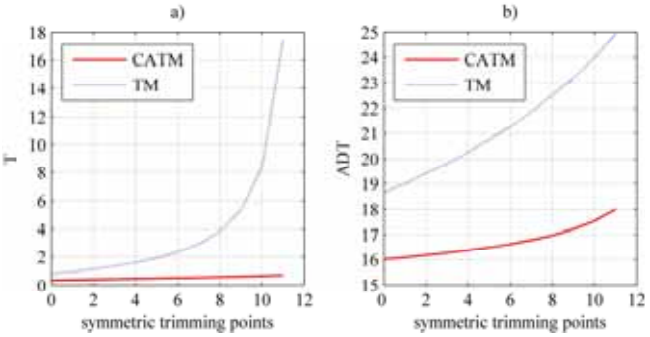


**Figure 7.** Scaling factor of the detection threshold $T$ and the average decision threshold $ADT$ of TM-CFAR and CATM-CFAR for symmetric trimming ($P_{fa}$=$10^{-6}$, $N$=24)

The notations CATM($T_1$,$T_2$) and TM($T_1$,$T_2$) stand for CATM-CFAR and TM-CFAR respectively with lower trimming $T_1$ and upper trimming $T_2$. The notation OS($k$) stands for the OS-CFAR where $k$ [7] is a well-known parameter of OS-CFAR which corresponds to the mentioned trimming value.

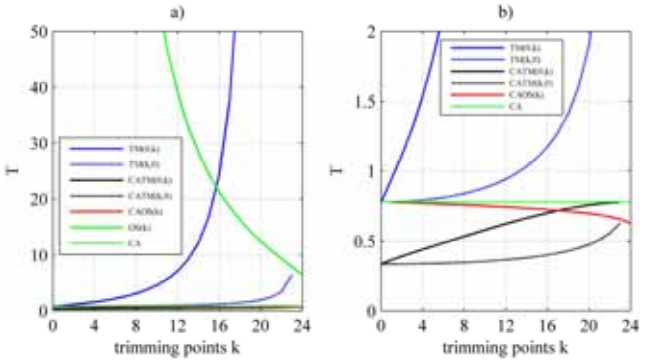


Figure 8. Scaling factor of the detection threshold $T$ of CA, OS, TM, CAOS and CATM-CFAR ($P_{fa}$=10$^{-6}$, $N$=24)

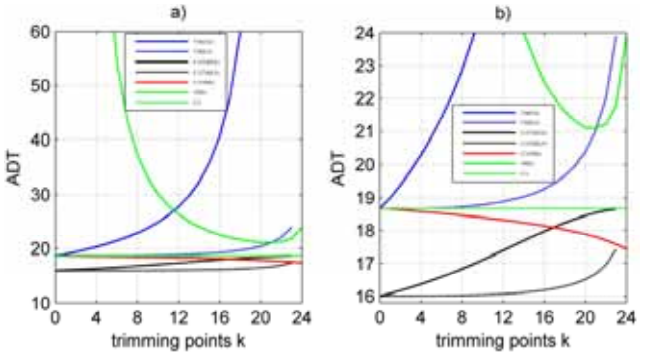


**Figure 9.** Average decision threshold $ADT$ of CA, OS, TM, CAOS and CATM-CFAR ($P_{fa}$=10$^{-6}$, $N$=24)

In general, for each trimming value $k$, the CATM-CFAR detector has $ADT$ values that are better than those for the TM, OS and CA-CFAR detectors.

## Simulation results

In this section, we carried out a simulation to prove practically good features of new CATM-CFAR detectors. We considered first simulated targets in Weibull clutter and then real targets in real clutter. The detection results of CA, TM, OS and CATM-CFAR are compared. The main parameters of the realized CFAR detectors are listed in Table 3. One model of the software radar receiver (SRR) is used for signal processing and target detection.

**Table 3.** Main parameters of the realized CFAR detectors

| model | $P_{fa}$ | $N$ | $T$ | $k$ | $T_1$ | $T_2$ |
|---|---|---|---|---|---|---|
| CA-CFAR | 10$^{-6}$ | 16 | 1.371 | - | - | - |
| TM-CFAR | 10$^{-6}$ | 16 | 2.377 | - | 2 | 2 |
| OS-CFAR | 10$^{-6}$ | 16 | 20.954 | 12 | - | - |
| CATM-CFAR | 10$^{-6}$ | 16 | 0.679 | - | 2 | 2 |

### *A) Used model of the SRR*

The main advantages of the software implementation of a radar receiver relative to hardware implementation are its adaptability in terms of changes in signal processing algorithms in the existing functional blocks, the possibility of easy implementation of new blocks with new features and less expensive maintenance. Therefore, we can use the model of the software radar receiver (SRR) presented in detail in [23], [25] and [26] and simply replace one CFAR block with another type of the CFAR block to get new detection results. The block diagram of the used SRR is shown in Fig.10. The SRR consists of only 64 reference cells per each azimuth. For this reason, the reference window in the CFAR block has a maximum of 16 reference cells. The A/D conversion is performed using a PCI-9812/10 acquisition board with four A/D channels with a maximum sampling rate of 20 Msamples/s on each channel. The I and Q outputs are A/D converted by 2 Msamples/s., Synchronization impulses from the PRF generator and the "impulses of north" are also A/D converted on the third and the fourth channel. The next unit is RANGE BIN memory in which the data from the A/D converter are stored and prepared for processing in the following units. This memory contains data packets from I and Q outputs and it has a form of a matrix. Each row contains I and Q samples from the same range bin and each column contains I and Q samples from a transmitted impulse. This matrix is generated for each antenna position per azimuth. A Doppler filter is realized as a third-order transversal filter. The filter coefficients are 1-2 and 1. Filtering is done on data vectors from the same range bin. The output of the envelope detector is further processed in the CFAR unit in accordance with the used algorithm. The target center per azimuth and range is calculated in the extractor. Otherwise, the indicator is panoramic and the detected targets are shown as light points, after each antenna rotation [27].

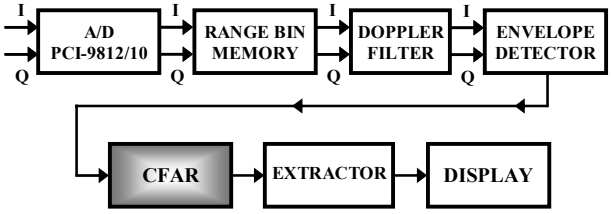


**Figure 10.** Block diagram of the used software radar receiver

### *B) Simulated targets in Weibull clutter*

First we simulated a group of three neighborhood targets per azimuth and range. The distance between two adjacent targets is only one radar resolution cell per range. So, it is quite difficult to detect all of them by many CFAR algorithms since they interfere strongly with each other. The target parameters are listed in Table 4. The targets have different $SNR$ and different speeds which are determined by the appropriated Doppler frequency $f_d$. The targets have a similar range $R$ for this model of the SRR and approximately the same azimuth . Also, Weibull clutter power is increased to the maximum value in order to identify the benefits of the CATM-CFAR detector.

**Table 4.** Parameters of the simulated radar targets in Weibull clutter

| target | $SNR$ [dB] | $f_d$ [Hz] | $R$ [km] | $\theta$ [deg] |
|---|---|---|---|---|
| 1 | 12.5 | 2500 | 8.9 | 198.9 |
| 2 | 17.5 | 3000 | 10.8 | 200.7 |
| 3 | 7.2 | 3500 | 12.6 | 199.5 |

A raw video signal for one antenna revolution is shown in Fig.11a. Three neighborhood targets can be observed more clearly in Fig.11b, selected per azimuth.

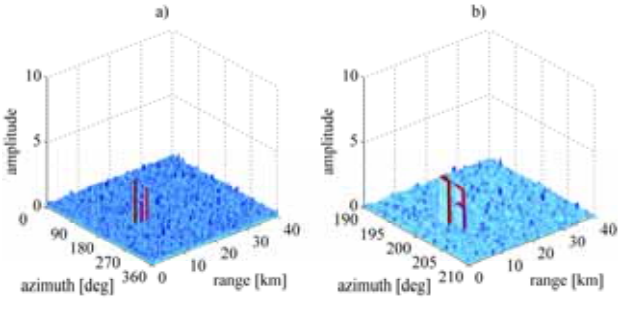


**Figure 11**. Raw video signal with the simulated targets in Weibull clutter

The result of the signal processing in the CA-CFAR detector is shown in Fig.12. It detects all three targets but there are many false targets in the displayed area. The radiogram of the CA-CFAR processing is shown in Fig.13.

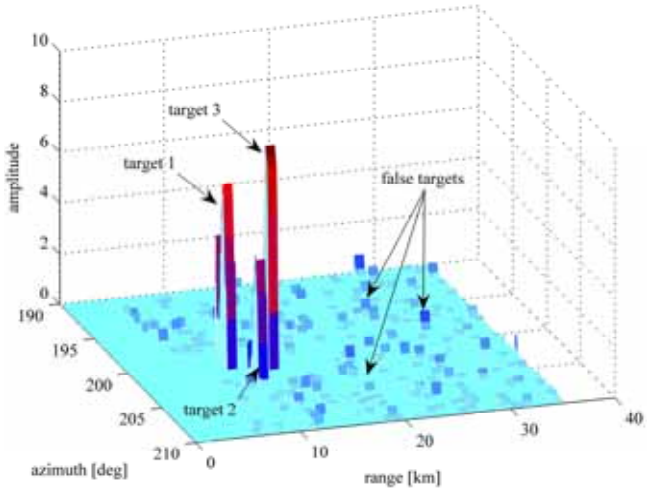


**Figure 12.** Result of the CA-CFAR processing

The result of signal processing in the TM-CFAR detector is shown in Fig.14. The TM-CFAR detects only the first and second target from Table 4. The radiogram of the TM-CFAR processing is shown in Fig.15.

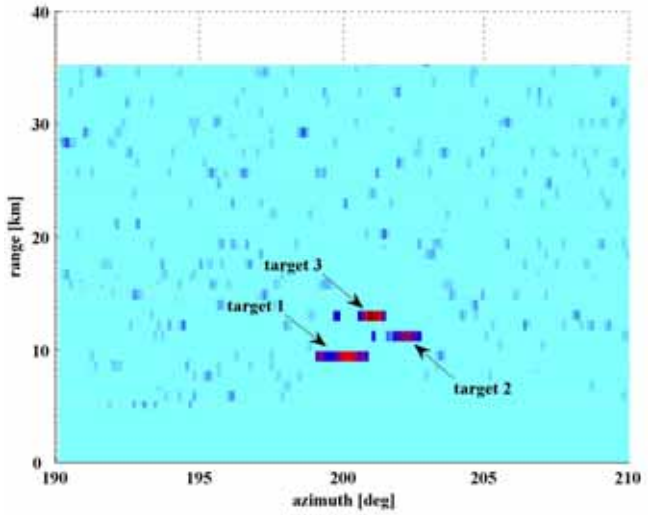


**Figure 13.** Radiogram of the CA-CFAR processing

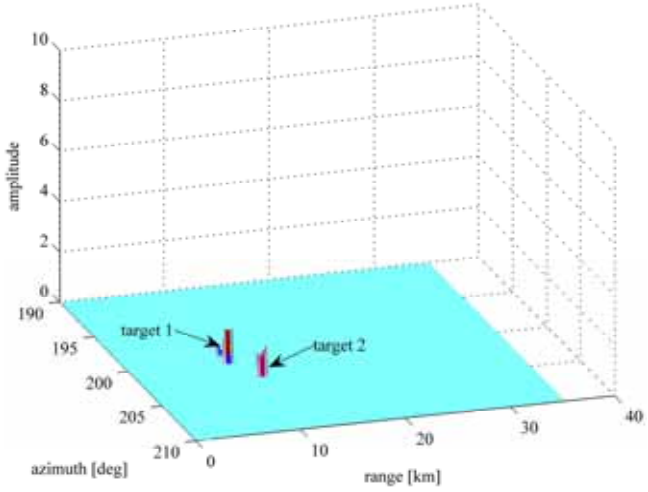


**Figure 14.** Result of the TM-CFAR processing

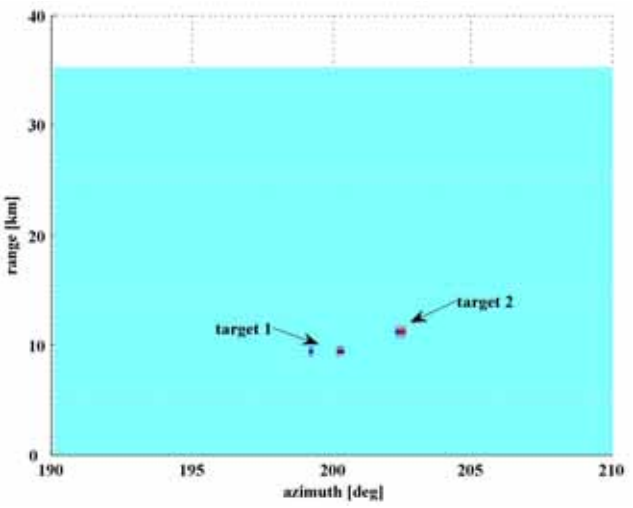


**Figure 15.** Radiogram of the TM-CFAR processing

However, the OS-CFAR detector gives good results. It detects all three neighbourhood targets with somewhat smaller amplitudes (Fig.16). The amplitude of target 2 is the smallest. We can see that TM and OS-CFAR detectors do not produce false targets. The radiogram of the OS-CFAR processing is shown in Fig.17.

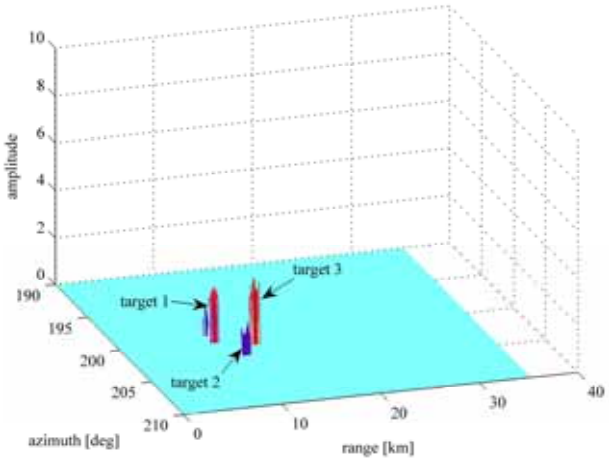


**Figure 16.** Result of the OS-CFAR processing

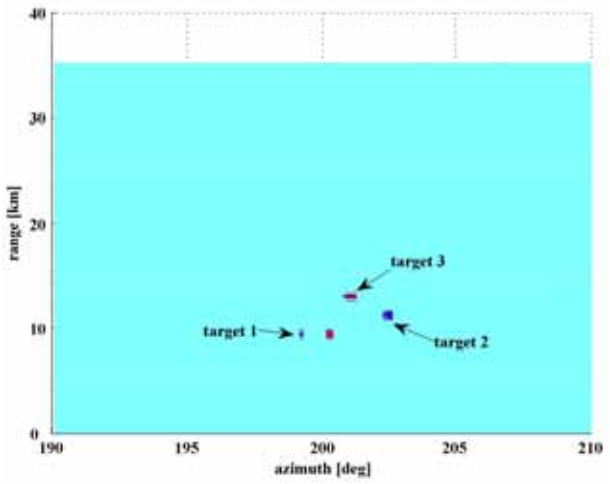


**Figure 17.** Radiogram of the OS-CFAR processing

The result of the new CATM-CFAR detector is shown in Fig.18. Three neighbourhood targets are easily visible and have the largest amplitudes compared to the previous three CFAR models. Also, there are no false targets. The radiogram of the CATM-CFAR processing is shown in Fig.19.

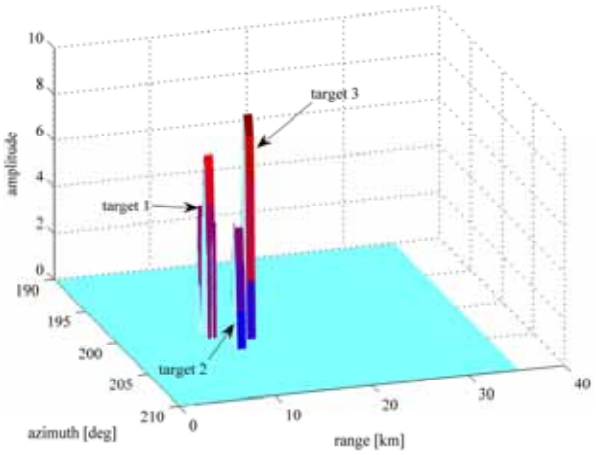


**Figure 18.** Result of the CATM-CFAR processing

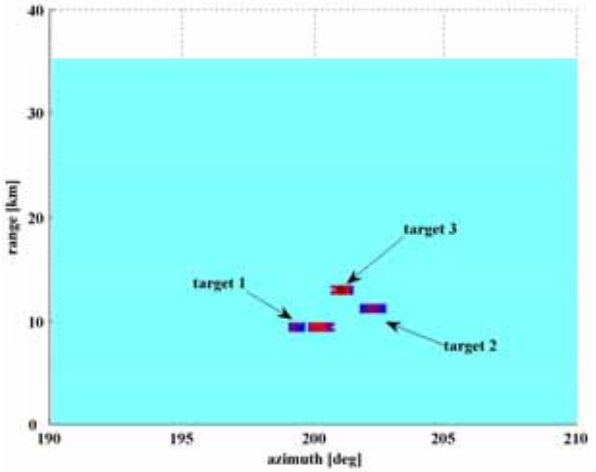


**Figure 19.** Radiogram of the CATM-CFAR processing

*C) Real targets in real clutter*

We also checked of the CATM-CFAR by detecting three real targets in real clutter. We used the PCI-9812/10 card (Fig.10) for the analog-to-digital (A/D) conversion of signals from I and Q branches of one real radar device. The sampling frequency was 2 MHz. The transmitted pulse power of the radar device was 15 KW, the frequency was 5.4 GHz, the pulse length was 6 μs, the pulse repetition frequency was 2350 Hz, the intermitted frequency was 30 MHz, the antenna scan rate was 1 Hz and the horizontal antenna beam width was 2.1. After A/D conversion follows the creation of the range bin memory. Then signals are processed in the Doppler filter. The output signal from the envelope detector is shown in Fig.20. This is a raw video signal for one antenna revolution in real clutter.

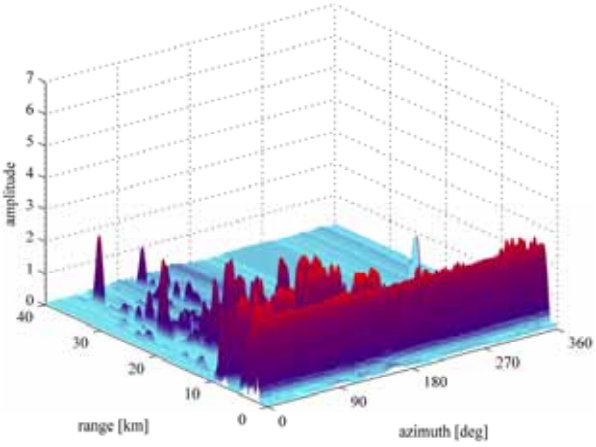


**Figure 20**. Raw video signal with real targets in real clutter

Present real targets cannot be seen in the raw video signal. After signal processing in the CA-CFAR detector, we can see three real targets and some false targets in Fig.21. The extractor of the used SRR model determined their coordinates. The coordinates of the detected real targets are shown in Table 5. The radiogram of the CA-CFAR processing is shown in Fig.22.

**Table 5.** Coordinates of real radar targets in real clutter

| target | $R$ [km] | $\theta$ [deg] |
|---|---|---|
| 1 | 7.3 | 54 |
| 2 | 12.4 | 71 |
| 3 | 6.1 | 229 |

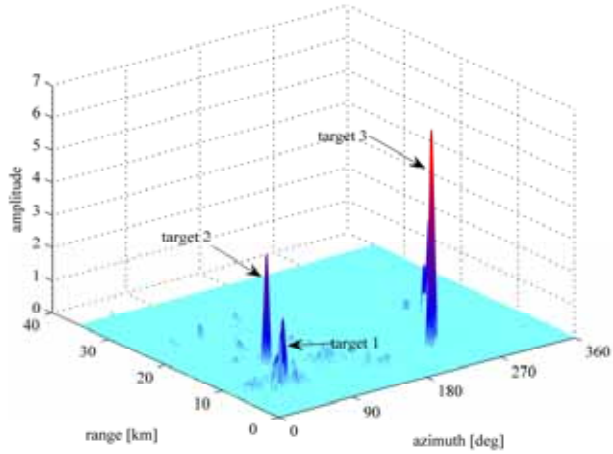


**Figure 21.** Result of the CA-CFAR processing for real targets in real clutter

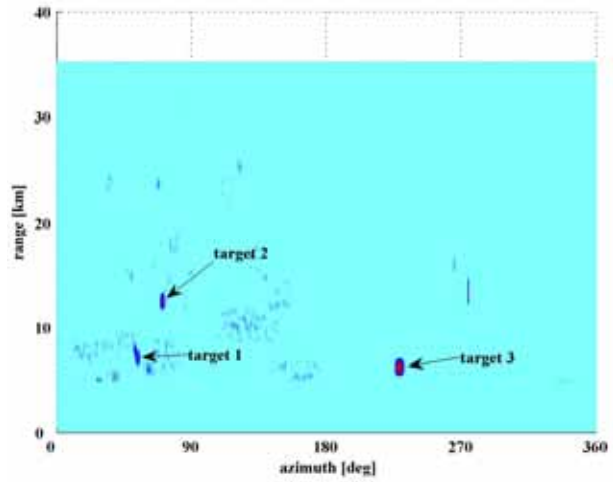


**Figure 22.** Radiogram of the CA-CFAR processing for real targets in real clutter

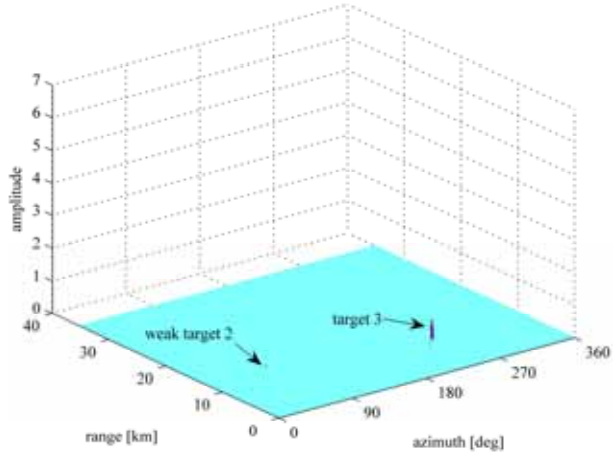


**Figure 23.** Result of the TM-CFAR processing for real targets in real clutter

The result of the signal processing in the TM-CFAR detector is shown in Fig.23. The TM-CFAR detects only the second and third target from Table 5. However, the detection of target 2 is very weak. The radiogram of the TM-CFAR processing is shown in Fig.24.

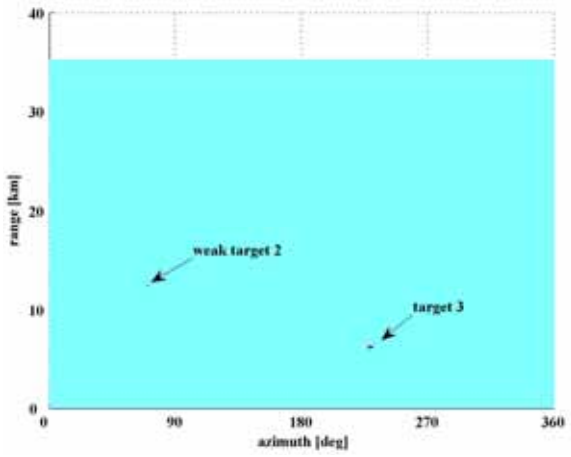


**Figure 24.** Radiogram of the TM-CFAR processing for real targets in real clutter

The OS-CFAR detector gives better results than the TM-CFAR detector. It detects all three real targets (Fig.25). However, the amplitude of target 1 is the smallest and within the detection limit. We have to emphasize here that the detection of target 1 would have been unsuccessful if its signal-to-noise ratio had been slightly lower. This statement is true for target 2 detection using the TM-CFAR algorithm. Also, we can see that TM and OS-CFAR detectors do not produce false targets again. The radiogram of the OS-CFAR processing is shown in Fig.26.

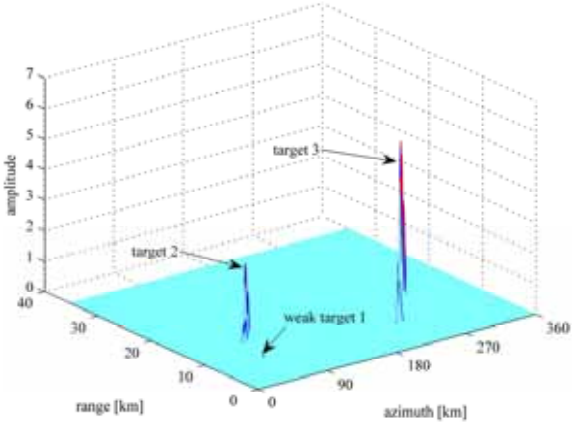


**Figure 25.** Result of the OS-CFAR processing for real targets in real clutter

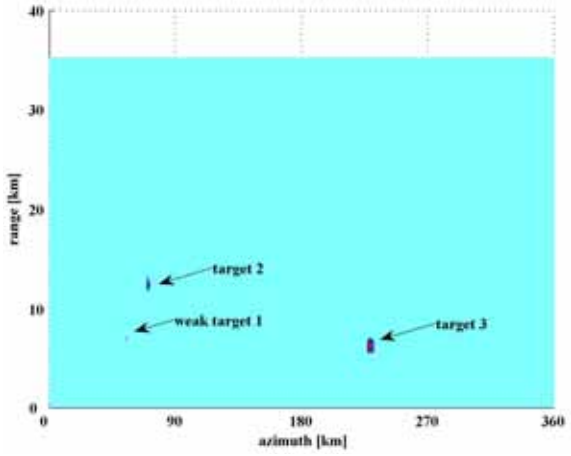


**Figure 26.** Result of the OS-CFAR processing for real targets in real clutter

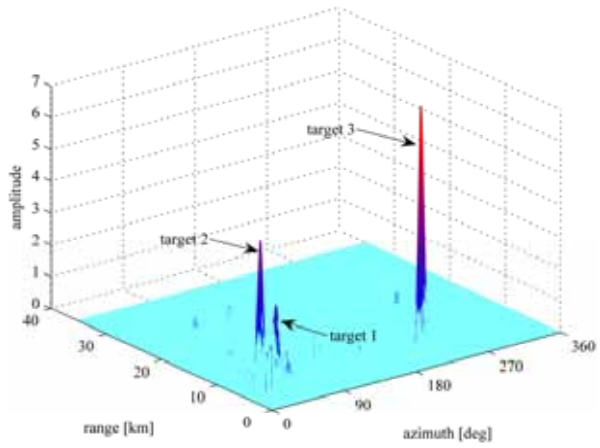


**Figure 27.** Result of the CATM-CFAR processing for real targets in real clutter

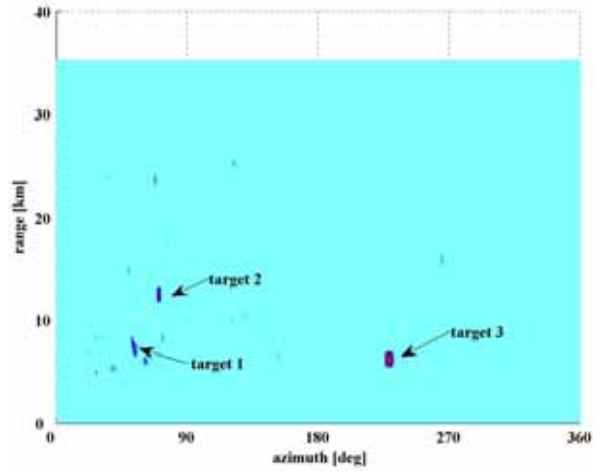


**Figure 28.** Radiogram of the CATM-CFAR processing for real targets in real clutter

The result of the detection of real targets in real clutter of the proposed CATM-CFAR detector is shown in Fig.27. Three real targets are easily visible and have the largest amplitudes compared to the previous three CFAR models. However, in this situation, we have some false targets because of real clutter fluctuation. The radiogram of the CATM-CFAR processing is shown in Fig.28.

## Conclusion

This paper presents an improvement of neighborhood targets detection in clutter environment. It is achieved by the CATM-CFAR detector. A fusion of particular decisions of the internal CA-CFAR and TM-CFAR algorithms within the CATM-CFAR detector provides a better final decision and detection. The advantage of using the CATM-CFAR detector is shown in the situation of detection of real targets in real clutter as well. Other realized detectors were then on the limit of a successful detection, or had a lot of false targets. All analyzed models of CFAR detectors in the article are supported using the MATLAB® software.

We derived the expressions for the probability of detection, the probability of false alarm and the average decision threshold of the CATM-CFAR and compared its performances with the performances of several other well-known CFAR detectors. Also, we derived a new expression for an approximate signal-to-noise ratio loss measured in dB which can be used for all CFAR models.

A direction of further research would be moving towards an examination of the characteristics of the realized CATM-CFAR detector under the conditions of jamming signal presence and its effect on the detection of radar targets.

## Acknowledgements

This work was partially supplied by the Ministry of Education, Science and Technological Development of the Republic of Serbia under Grants III-47029 (2011.-2015.).

## References

[1] FINN,H.M., JOHNSON,R.S.: *Adaptive detection mode with threshold control as a function of spatially sampled clutter level estimate*, RCA Rev., 1968, 29, (3), pp.414–464.

[2] TRUNK,G.V.: *Range resolution of targets using automatic detectors*, IEEE Trans. Aerosp. Electron. Syst., 1978, 14, (5), pp.750–755.

[3] HANSEN,G.V., SAWYERS,J.H.: *Detectability loss due to greatest-of selection in a cell averaging CFAR*, IEEE Trans. Aerosp. Electron. Syst., 1980, 16, pp.115–118.

[4] GOLDMAN,H., BAR-DAVID,I.: *Analysis and application of the excision CFAR detector*, IEE Proc. Radar Sonar Navig., 1988, 135F, pp.563–575.

[5] GOLDMAN,H.: *Performance of the excision CFAR detector in the presence of interferers*, IEE Proc. Radar Sonar Navig., 1990, 137F, (3), pp.163–171.

[6] RICKARD,J.T., DILLARD,G.M.: *Adaptive detection algorithms for multiple target situations* , IEEE Trans. Aerosp. Electron. Syst., 1977, 13, (4), pp.338–343.

[7] ROHLING,H.: *Radar CFAR thresholding in clutter and multiple target situations*, IEEE Trans. Aerosp. Electron. Syst., 1983, 19, pp.608–621.

[8] GANDHI,P.P., KASSAM,S.A.: *Analysis of CFAR processors in nonhomogenous background*, IEEE Trans. Aerosp. Electron. Syst., 1988, 24, (4), pp.427–445.

[9] KIM,C.J., LEE,H.S.: *Detection analysis of generalized order statistics CFAR detector for correlated Rayleigh target*, Elsevier Science, Signal Processing, 1995, 47, pp.227–233.

[10] BARKAT,M., DIB,S.: *CFAR detection for two correlated targets*, Elsevier Science, Signal Processing, 1997, 61, pp.289–295.

[11] FARROUKI,A., BARKAT,M.: *Automatic censoring CFAR detector based on ordered data variability for nonhomogenous environments*, IEE Proc. Radar Sonar Navig., 2005, Vol.152, No.1, pp.43–51.

[12] FARROUKI,A., BARKAT,M.: *Automatic censored mean level detector using a variability-based censoring with non-coherent integration*, Elsevier Science, Signal Processing, 2007, 87, pp.1462–1473.

[13] ELIAS,A.R., GARSIA,G.M.: *Analysis of some modified ordered statistic CFAR: OSGO and OSSO CFAR*, IEEE Trans. Aerosp. Electron. Syst., 1990, 26, (1), pp.197–202.

[14] EL MASHADE,M.B.: *Performance analysis of modifed ordered-statistics CFAR processors in nonhomogenous environments*, Elsevier Science, Signal Processing, 1995, 41, pp. 379–389.

[15] ZAIMBASHI,A., TABAN,M.R. NAYEBI,M.M., NOROUZI,Y.: *Weighted order statistic and fuzzy rules CFAR detector for Weibull clutter*, Elsevier Science, Signal Processing, 2008, 88, pp.558–570.

[16] GOWDA,C.H., UNER,M.K., VARSHNEY,P.K., VISWANATHAN,R.: *Distributed CFAR target detection*, Journal of the Franklin Institute, 1999, 336, pp.257–267.

[17] HAMMOUDI,Z., SOLTANI,F.: *Distributed CA-CFAR and OS-CFAR detection using fuzzy spaces and fuzzy fusion rules*", IEE Proc. Radar Sonar Navig., 2004, Vol.151, No.3, pp.135–142.

[18] LATIFA,A.: *A novel optimization method for dependent CFAR detection*, Journal of Electrical and Electronics Engineering, 2011, Vol.4, No.2, pp.11–16.

[19] MEZIANI,H.A., SOLTANI,F.L *Decentralized fuzzy CFAR detectors in homogenous Pearson clutter background*, Elsevier Science, Signal Processing, 2011, 91, pp.2530–2540.

[20] EL MASHADE,M.B.: *Detection analysis of linearly combined order statistic CFAR algorithms in nonhomogeneous background environments*, Elsevier Science, Signal Processing, 1998, 68, pp.59–71.

[21] ZHAO,L., LIU,W., WU,X., FU,J.S.: *A novel aproach for CFAR processors design*, Proc. of the IEEE International Conference on Radar, Atlanta, GA, 1-3 May 2001, pp.284–288.

[22] ESTRADA,S.L., CUMPLIDO,R.: *Fusion center with neural network for target detection in background clutter*, Proc. of the Sixth Mexican International Conference on Computer Science (ENC'05), 2005.

[23] IVKOVIC,D., ZRNIC,B., ANDRIC,M.: *Fusion CFAR detector in receiver of the software defined radar*, Proc. of the International Radar Symposium IRS-2013, Dresden, Germany, 19-21 June 2013.

[24] PAPOULIS,A.: *Probability, Random Variables and Stochastic Processes*, McGraw-Hill, New York, USA, 1984.

[25] IVKOVIC,D., SIMIC,S., DUKIC,M., ERIC,M.: *Design and Implementation of Software Defined Receiver in a Conventional Radar*, Proc. of the International Radar Symposium IRS-2005, Berlin, Germany, 2005.

[26] IVKOVIC,D., SIMIC,S., DUKIC,M., ERIC,M.: *Software model of the Signal Processing Unit in the Conventional Radar*, Proc. of the EUROCON, Belgrade, Serbia, 2005.

[27] MALJKOVIĆ,M., SAJNKAR,V.L., DELEVIĆ,M., KOROLIJA,D.: *Softvare defined radio*, KumNTI 3/2008, ISSN 1820-3418, ISBN 978-86-81123-28-7, Military Technical Institute, Belgrade, Serbia, 2008, Vol.XLII, No.3.

Received: 24.11.2014.

# CATM-CFAR detektor u prijemniku softverski definisanog radara

**U ovom radu predstavljen je model CATM-CFAR detektora u prijemniku softverski definisanog radara. Pomenuti detektor predstavlja kombinaciju CA i TM CFAR detektora. On je implementiran u prijemnik softverski definisanog radara. U ovom radu su prikazani određeni rezultati istraživačkog rada na dizajniranju i implementaciji softverskog radarskog prijemnika konvencionalnog radara. Izvedeni su izrazi za verovatnoću detekcije, verovatnoću lažnog alarma i srednji prag detekcije za CATM-CFAR detektor. Prikazani su rezultati detekcije simuliranih radarskih ciljeva u Vejbulovom klateru i detekcije realnih radarskih ciljeva u realnom klateru. Izvršena je komparativna analiza karakteristika novog CATM-CFAR detektora sa određenim dobro poznatim CFAR detektorima.**

*Ključne reči*: **detektor, detekcija, radar, akvizicija cilja, klater, prijemnik, softverski definisani radar.**

# Детектор Chatham-CFAR в приёмнике радара определённого программным обеспечением

**В этой статье мы представляем модель Chatham-CFAR детектора в приёмнике радара определённого программным обеспечением. Вышеупомянутый датчик представляет собой комбинацию CA и TM CFAR детектора. Он был реализован в приёмнике радара определённого программным обеспечением. В этой статье приведены некоторые результаты исследований по разработке и реализации приёмника обычного традиционного радара определённого**

**программным обеспечением. Получены выражения для вероятности обнаружения, для вероятности ложной тревоги и среднего порога обнаружения для детектора Chatham-CFAR. Тоже показаны результаты обнаружения моделируемых радиолокационных целей в клаттере Вейбулла и обнаружения реальных помех и радиолокационных целей в режиме реального клаттера. Проведён сравнительный анализ характеристик нового детектора Chatham-CFAR с некоторыми хорошо известными детекторами CFAR.**

*Ключевые слова:* **детектор, детекция, радар (РЛС), целеуказание, клаттер, приёмник, радар определённый программным обеспечением.**

# Détecteur CATM-CFAR dans le récepteur du radar défini par logiciel

**Le modèle du détecteur CATM-CFAR dans le récepteur du radar défini par logiciel est présenté dans ce papier. Le détecteur cité représente la combinaison des détecteurs CA et TM CFAR. Il a été installé dans le récepteur du radar défini par logiciel. Dans ce papier on a présenté certains résultats des recherches sur le dessin et l'installation du récepteur du radar défini par logiciel d'un radar conventionnel. On a dérivé les expressions pour la probabilité de détection de la fausse alarme et le seuil moyen de détection pour le détecteur CATM-CFAR. On a présenté les résultats de la détection des cibles radar simulées dans le clutter de Weibull et de la détection des cibles radar réelles dans le clutter réel. Une analyse comparative entre le caractère du nouveau détecteur CATM-CFAR et les détecteurs CFAR déjà bien connus a été faite aussi.**

*Mots clés:* **détecteur, détection, radar, acquisition de cible, clutter, récepteur, radar défini par logiciel.**